NANO LETTERS

pubs.acs.org/NanoLett

Correlation between Incident and Emission Polarization in Nanowire Surface Plasmon Waveguides

Zhipeng Li,[†] Kui Bao,[‡] Yurui Fang,[†] Yingzhou Huang,[†] Peter Nordlander,[†,‡,*] and Hongxing Xu[†,§,*]

[†]Beijing National Laboratory for Condensed Matter Physics, and Institute of Physics, Chinese Academy of Sciences, Box 603-146, 100190, Beijing, China, [‡]Department of Physics and Astronomy, Department of Electrical and Computer Engineering, Laboratory for Nanophotonics, Rice University, Houston, Texas 77005, and [§]Division of Solid State Physics/The Nanometer Consortium, Lund University, Box 118, S-22100, Lund, Sweden

ABSTRACT Nanowire plasmons can be launched by illumination at one terminus of the nanowire and emission can be detected at the other end of the wire. Using polarization dependent dark-field scattering spectroscopy, we measure how the polarization of the emitted light depends on the polarization of the incident light. We observe that the shape of the nanowire termination plays an important role in determining this polarization change. Depending on termination shape, a nanowire can serve as either a polarization-maintaining waveguide, or as a polarization-rotating, nanoscale half-wave plate. The understanding of how plasmonic waveguiding influence the polarization of the guided light is important for optimizing the structure of integrated plasmonic devices.

KEYWORDS Nanowire, plasmonics, waveguide, polarization

Subwavelength photonic devices can be integrated with electronics to overcome the bandwidth and data transmission rate limitations of classical electrical interconnects.[1] The development of such miniaturized photonic circuits is of great current interest in nanophotonics.[2,3] Plasmonics as a subfield of nanophotonics is concerned with the control of light at the nanoscale, using surface plasmons polaritons (SPPs).[4−11] As the nanoscale analog of an optical fiber, plasmonic waveguides are an important component needed for light transmission in surface plasmon-based photonic circuitry.[12−14] Recently various types of plasmonic waveguides have been developed.[15−19] It has been shown that gold and silver nanowires can guide SPPs up to tens of micrometers with relative low loss of energy.[20−28] Many studies have focused on improving the performance of the nanowire waveguide, achieving higher in-coupling efficiency of light[23,28] and lower propagation loss.[8,24] However, very little is known about how the polarization of the out-coupled light is related to the polarization of the incident light. An understanding of the input-output polarization properties of light from plasmonic nanowire waveguides is crucial for waveguide design, optical interconnects, and the ultimate integration of active plasmonic devices such as logic elements, switcher, and multiplexers.

In this paper, SPPs are excited at one end of a silver nanowire. While varying the polarization of the excitation beam, the polarization of the light emitted at the other end of the nanowire was analyzed. The polarization change is found to depend sensitively on the geometrical shape of the wire terminations. Theoretical analysis shows that the shape of the nanowire termination where the plasmon is launched determines the relative intensity of the SPPs modes excited in the nanowire, which can modify the polarization of the emitted light. The shape of the emission end, on the other hand, can change both the spatial distribution and polarization of the emitted light. With properly designed nanowire terminations, a nanowire can serve either as a polarization-maintaining plasmonic waveguide or as a nanoscale polarization rotating half-wave plate.[29,30]

The experimental setup is shown in Figure 1a. A laser beam with the wavelength 633 nm is focused onto one end of a silver nanowire with an objective (Olympus UPlanApo, 100×, N.A. = 1.35). The polarization of the incident light is rotated by a half-wave plate before the half-reflecting mirror. The emission from the other end of the nanowire is collected by the same objective and recorded by a TE cooled 1392 × 1040 CCD detector. By rotating the polarizer in front of the CCD detector, the polarization of the light emitted from the nanowire can be obtained. The silver nanowires were synthesized by chemical fabrication, which yields highly crystalline nanowires with smooth surfaces.[31] The wires are deposited on an ITO glass substrate and immersed in index matched oil $n = 1.518$ during the measurement.

Figure 1b shows the transmission electron microscopy (TEM) image of an Ag nanowire of length 3.36 μm and diameter 130 nm. The shape of the nanowire ends are shown with increased detail in the insets. The angle α and

* To whom correspondence should be addressed. E-mail: (H.X.X) hxxu@iphy.ac.cn; (P.N) nordland@rice.edu.

Received for review: 02/12/2010
Published on Web: 04/06/2010

DOI: 10.1021/nl100528c | *Nano Lett.* **2010,** *10,* 1831–1835

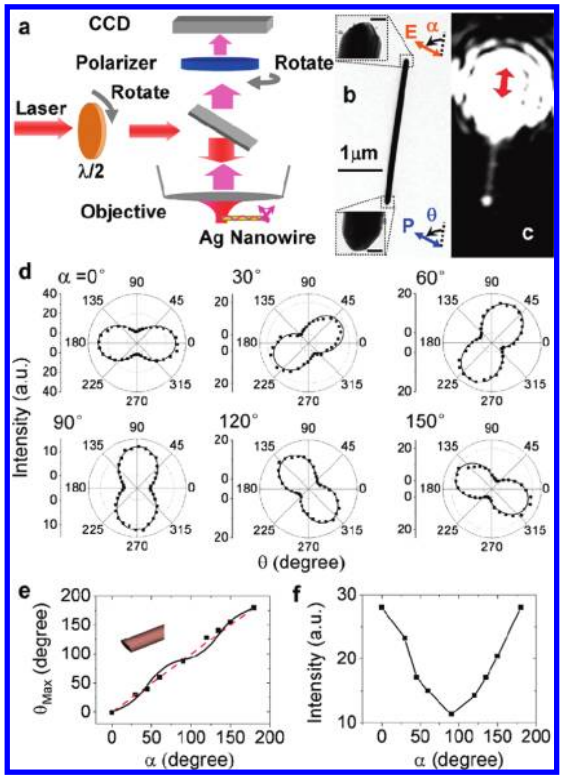

FIGURE 1. Polarization measurement. (a) Scheme of the experiment. (b) TEM image of a wire of length 3.36 μm and diameter 130 nm. The scale bar in the TEM insets showing the shape of the wire ends is 50 nm. (c) Optical image of the nanowire in a microscope under the excitation of a 633 nm laser spot polarized along the wire. Red arrow indicates the polarization of the laser. (d) Emission intensity as a function of the polarizer rotation angle θ, for different incident polarizations ($\alpha = 0$, 30, 60, 90°, 120, and 150°, respectively). The incident polarization and the polarizer are rotated anticlockwise relative to the wire axis, which is defined by the angle α and θ in the inset of (b). (e) Polarization of the emission as a function of the incident polarization. θ_{max} is the polarization angle of the emission defined as the rotation angle of the polarizer when the emission is the maximum. Dots are the measured data. Black curve is the simulation result based on a cylindrical wire with the shape of both ends shown in the inset. The linear dashed red line is drawn to guide the eyes. (f) Maximum emission intensity from the wire as a function of incident polarization angle.

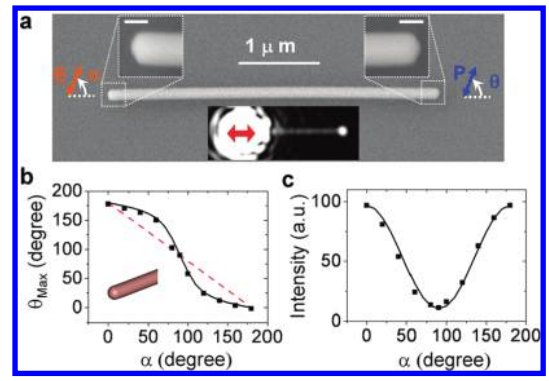

FIGURE 2. Polarization of emitted light from nanowires. (a) Scanning electron microscopy image of a wire of length 4.54 μm and diameter 148 nm. The scale bar in the insets showing the wire ends is 100 nm. The incident polarization and the polarizer are rotated anticlockwise relative to the wire axis. Inset below: optical image of the wire excited by a parallel polarized 633 nm laser spot at the left end resulting in light emission from the other end of the wire. The red arrow indicates the polarization of the laser. (b) Polarization of the emission as a function of the incident polarization. θ_{Max} is the polarization angle of the emitted light. Dots are the measured data. Black curve is the simulation result based on a cylindrical wire with the shape of both terminations shown in the inset. The linear red line is drawn to guide the eyes. (c) Maximum emission intensity from the wire under different the incident polarizations.

θ correspond to the incident polarization and the rotation of the polarizer, respectively. Both angles are rotated anticlockwise relative to the wire axis. In Figure 1c, a bright emission spot can be observed following excitation of SPPs from the incident wire end. Figure 1d shows the intensity of the wire emission as a function of the rotation of the polarizer. It is clear that nanowire emission as a function of incident polarization angle is almost always linearly polarized. Hence, the direction of the emission polarization can be defined as the angle θ_{Max} when the polarizer is rotated to the emission intensity maximum. The angle θ_{Max} as a function of the incident polarization is shown in Figure 1e. Here we observe that the emission polarization is proportional to the incident polarization, which means that the nanowire SPPs in this case are polarization-maintaining. In this nanowire, parallel incident polarization ($\alpha = 0°$) results in a 2.5 times larger emission intensity than in the case of perpendicular incident polarization ($\alpha = 90°$) (Figure 1f).

The result for another wire is shown in Figure 2. The wire has a similar length (4.54 μm) and diameter (148 nm) to the one in Figure 1b, but has different end shapes (see the scanning electron microscopy images in Figure 2a). As shown in Figure 2b, the polarization of the emitted light still depends on the incident polarization. Interestingly, θ_{Max} decreases as the incident polarization α increases, which is opposite to the case in Figure 1. The emission intensity under different excitation polarizations is shown in Figure 2c. Here, parallel excitation results in ~9 times stronger wire emission than for the perpendicular case.

To understand the polarization rotation properties of these nanowires, we performed electromagnetic calculations using finite element method (FEM)-based commercial software (COMSOL). We simulated nanowires with the same length and diameter as those in our experiment, successfully reproducing the measured results. This is shown by the black curves in Figures 1e and 2b, where the shapes of the ends of the simulated nanowires are shown in the inset. The terminations of chemically synthesized crystalline nanowires usually have five {111} facets.[31] Although we cannot precisely reconstruct the shape of the nanowire ends with high accuracy from electron microscopy images, simulations indeed confirm that within a certain range of wire lengths, it is the shape of the nanowire terminations and not the length of the nanowire that determines the polarization of the emitted light. All the termination shapes used in the simulations presented in this paper are consistent with the SEM images.

DOI: 10.1021/nl100528c | Nano Lett. 2010, 10, 1831–1835

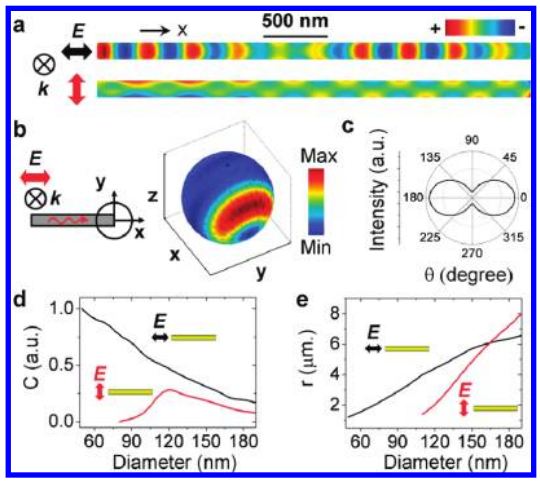

FIGURE 3. SPPs modes in wires with flat terminations. (a) Charge distribution on the surface of a wire of the length 3.36 μm and diameter 130 nm with flat ends. The left end is excited by a 633 nm focused beam with polarization parallel and perpendicular to the wire, respectively. Colors from red to blue represent charges from positive to negative. (b) The resultant spatial distribution of the emission intensity on a sphere enclosing the wire end excited by the parallel incident polarization. Colors and black lines represent the intensity and the polarization of the emission on the sphere. (c) Emission polarization from the wire excited under the parallel polarized excitation. (d) The in-coupling efficiency C for two SPPs modes (black curve for $m = 0$ mode, red curve for $m = 1$ mode) as a function of the wire diameter. (e) The $1/e$ damping length r of both modes as a function of the wire diameter.

To illustrate the relation between the emission polarization and the shape of the nanowire termination, we first consider a cylindrical nanowire with flat ends. Figure 3a shows the charge distribution on the surface of a cylindrical wire with excitation at the left end of the nanostructure. For parallel incident polarization, the fundamental $m = 0$ SPP mode is excited in the wire. For a given position along the wire, the charge density associated with this mode is uniform around the azimuth of the wire. The resulting spatial distribution of the emission intensity on a sphere enclosing the wire end is shown in Figure 3b (enlarged view in Supporting Information). The $m = 0$ mode will result in parallel polarized emission from the right termination, shown in Figure 3c. For perpendicular incident polarization, a transverse charge oscillation is excited, corresponding to the $m = 1$ wire SPP mode. For a given position along the nanowire, the charge density distribution associated with this mode has two nodes around the nanowire azimuth, resulting in a perpendicularly polarized wire emission (not shown). For arbitrary incident polarization, both modes can be excited in the wire, and the polarization of the emitted light is determined by a superposition of emission from the $m = 0$ and $m = 1$ SPP modes. Hence, in any specific nanowire, the polarization of the emitted light is dependent on the relative in-coupling efficiency to the SPP modes and on the damping rate of each mode. By calculating the energy flow of the SPPs excited by the parallel and perpendicular polarization, we fit an exponentially damped energy flow with the formula $Ce^{-x/r}$, where C is the coupling efficiency and r is the $1/e$ damping length of an SPP, respectively, where x is the distance from the excitation end. For nanowires with diameters D larger than 120 nm, the in-coupling efficiency for the $m = 0$ mode decreases monotonically with increasing D, a result which also has been found by other groups in studies of the coupled dipole-wire system.[32,33] The in-coupling efficiency for the $m = 1$ mode (red curve) peaks at $D = 120$ nm and then decreases with decreasing D. This decrease in the coupling for thin wires is caused by the effective cut off of the $m = 1$ modes for thin wires where their effective mode volume becomes much larger than the nanowire.[33] The $1/e$ damping length increases monotonically with increasing D for both the $m = 0$ and $m = 1$ modes due to less dissipation for thicker metallic nanowires.[33] The damping length of the $m = 1$ mode increases more rapidly than the $m = 0$ mode (Figure 3e). For wires with $D < 160$ nm, the $m = 0$ mode is less damped than the $m = 1$ mode. For this reason, excitation with parallel polarization will result in stronger light emission than excitation with perpendicular polarization as shown in Figure 2c. This polarization-dependent difference in emission intensity that favors the parallel mode is the reason for the nonlinear input−output polarization characteristic shown in Figure 2b. It is important to note that when D is 160 nm or larger, the $1/e$ damping lengths of both $m = 0$ and $m = 1$ modes are of the order of several micrometers. This means that for thick nanowires differing in lengths by several hundreds of nanometers, the relative intensities of the $m = 0$ and $m = 1$ SPP modes will be nearly the same, thus preserving the emission polarization.

The specific shape of the excitation end of the nanowire determines the relative intensity of the two SPP propagating modes, thus strongly affecting the emission polarization. For nanowires with an arbitrary termination shape, both plasmon modes can be excited for arbitrary polarizations. Figure 4a shows a three-dimensional (3D) view of the calculated charge distribution on the surface of a cylindrical nanowire with a 25° side-cut incident end excited by parallel polarized light. The charge plot shows that the resulting mode is a superposition of both $m = 0$ and $m = 1$ modes. The polarization of the emitted light is ~60° (shown in Figure 4b). Conversely, the shape of the emission end also influences the polarization of the emitted light. In Figure 4c, a wire with a flat incident end and a 60° side-cut emission end is excited by parallel polarized light. Just as shown in Figure 3a, only the $m = 0$ wire SPP mode is excited. Because of the asymmetric shape of the emission end, the spatial distribution of the emission intensity is asymmetric (enlarged view of Figure 4c in Supporting Information). The polarization of the emission is changed to −45° as shown in Figure 4d, rather than parallel to the wire axis. Further theoretical

DOI: 10.1021/nl100528c | *Nano Lett.* **2010,** *10,* 1831–1835

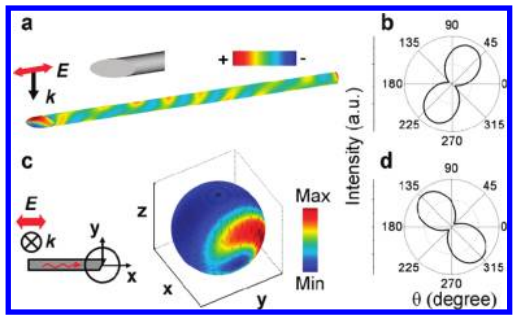

FIGURE 4. The effect of the termination shape of nanowires on the emission polarization. (a) A 3D view of the charge distribution on the wire surface under the excitation of a parallel polarized beam of wavelength 633 nm. The wire of the length 3.36 μm and diameter 130 nm has a 25° side-cut incident end and a flat emission end as shown in the inset. Colors from red to blue represent charges from positive to negative. (b) Polarization of the emission from the wire in (a) under the parallel polarized excitation. (c) Spatial distribution of the emission intensity on a sphere enclosing the wire end. The cylindrical wire has a flat incident end and a 60° side-cut emission end. The $m = 0$ mode is excited in the wire by a parallel polarized 633 nm laser at the left end. Colors and black lines represent the intensity and the polarization of the emission on the sphere. (d) Emission polarization from the wire in (c) excited under the parallel polarized excitation.

investigation on the emission polarization from wires with various shapes will be presented in a future study.

As demonstrated above, by modifying the shape of the incident wire end, one can control the relative intensities of the two SPP modes launched in the wire. The light emission characteristics will depend both on the relative intensities of the $m = 0$ and $m = 1$ modes reaching the emission end and on the shape of the emission wire terminus. Because of the mode-specific damping lengths of the SPPs, the properties of the emission polarization can depend on the wire diameter and for long wires, the wire length (Figure S4 in Supporting Information).

The present study clearly revealed that the major factor influencing the light emission polarization is the shape of the wire terminations. Although chemically synthesized crystalline nanowires usually has five {111} facets,[31] these facets are sometimes not identical, which leads to nanowire terminations of various multifaceted shapes. As a consequence, the emission polarization properties of each nanowire will depend on its particular shape. An extensive investigation of tens of nanowires (a few are presented in the Supporting Information) shows that most of them have emission polarization characteristics that either correlates positively with the incidence polarization (Figure 1 and Supporting Information Figure S2) or correlates negatively (Figure 2). In rare instances, the emission polarization depends on the incidence polarization in more complex way (Supporting Information Figure S3). To manipulate the polarization of the nanowire emission, we envision that one could reshape the nanowire terminations to desired shapes by techniques such as focused ion or electron beam milling. It is important to note that by controlling the shape of the nanowire terminations it will be possible to selectively fabricate polarization-maintaining or polarization-changing plasmonic waveguides in a controlled manner.

In conclusion, we have investigated the correlation between the incident and emission polarization in plasmonic Ag nanowire waveguides. By combining experiments and simulations, we find that the polarization change depends only slightly on the diameter and length of the wire, but sensitively on the shape of the wire terminations. The shape of incident nanowire end influences the strength of the SPP modes excited on the nanowire, while the shape of the emission end affects the intensity distribution and polarization of the emitted light. Hence, the polarization and intensity of the nanowire emission can be manipulated by modifying the shape of the nanowire termination. A polarization controllable nanoscale plasmonic waveguide may be useful in applications in nanophotonics,[2,12] such as chip-to-chip interconnects, or in specific applications, such as quantum cryptography.[34]

Acknowledgment. The authors acknowledge valuable discussions with Professor Naomi Halas and Dr. Feng Hao. This work was supported by NSFC Grant 10904171, 90923003, 10625418, 10874233, MOST Grant 2006DFB02020, 2009CB930700, "Bairen Project" of CAS, and the Robert A. Welch foundation under Grant C-1222, the National Science Foundation under Grant CNS-0421109, and by the U.S. Army Research Office under Grant W911NF-04-1-0203.

Supporting Information Available. Enlarged view of Figures 3b and 4c and more experimental measurements of the emission polarization from nanowires. This material is available free of charge via the Internet at http://pubs.acs.org.

REFERENCES AND NOTES

(1) Duan, X. F.; Huang, Y.; Cui, Y.; Wang, J. F.; Lieber, C. M. *Nature* **2001**, *409*, 66–69.
(2) Kirchain, R.; Kimerling, L. *Nat. Photonics* **2007**, *1*, 303–305.
(3) Guo, X.; Qiu, M.; Bao, J. M.; Wiley, B. J.; Yang, Q.; Zhang, X. N.; Ma, Y. G.; Yu, H. K.; Tong, L. M. *Nano Lett.* **2009**, *9*, 4515–4519.
(4) Raether, H. H. *Surface Plasmons*; Springer: Berlin, 1988.
(5) Xu, H. X.; Bjerneld, E. J.; Käll, M.; Börjesson, L. *Phys. Rev. Lett.* **1999**, *83*, 4357–4360.
(6) Ozbay, E. *Science* **2006**, *311*, 189–193.
(7) Bryant, G. W.; De Abajo, F. J. G.; Aizpurua, J. *Nano Lett.* **2008**, *8*, 631–636.
(8) Oulton, R. F.; Sorger, V. J.; Genov, D. A.; Pile, D. F. P.; Zhang, X. *Nat. Photonics* **2008**, *2*, 496–500.
(9) Neutens, P.; Van Dorpe, P.; De Vlaminck, I.; Lagae, L.; Borghs, G. *Nat. Photonics* **2009**, *3*, 283–286.
(10) Dorfmuller, J.; Vogelgesang, R.; Weitz, R. T.; Rockstuhl, C.; Etrich, C.; Pertsch, T.; Lederer, F.; Kern, K. *Nano Lett.* **2009**, *9*, 2372–2377.
(11) Schnell, M.; Garcia-Etxarri, A.; Huber, A. J.; Crozier, K.; Aizpurua, J.; Hillenbrand, R. *Nat. Photonics* **2009**, *3*, 287–291.
(12) Barnes, W. L.; Dereux, A.; Ebbesen, T. W. *Nature* **2003**, *424*, 824–830.
(13) Zia, R.; Schuller, J. A.; Chandran, A.; Brongersma, M. L. *Mater. Today* **2006**, *9*, 20–27.

DOI: 10.1021/nl100528c | *Nano Lett.* **2010,** *10,* 1831–1835

(14) Falk, A. L.; Koppens, F. H. L.; Yu, C. L.; Kang, K.; Snapp, N. D.; Akimov, A. V.; Jo, M. H.; Lukin, M. D.; Park, H. *Nat. Phys.* **2009**, *5*, 475–479.
(15) Lal, S.; Link, S.; Halas, N. J. *Nat. Photonics* **2007**, *1*, 641–648.
(16) Maier, S. A.; Kik, P. G.; Atwater, H. A.; Meltzer, S.; Harel, E.; Koel, B. E.; Requicha, A. G. *Nat. Mater.* **2003**, *2*, 229–232.
(17) Li, Z. P.; Xu, H. X. *J. Quant. Spectrosc. Radiat. Transfer* **2007**, *103*, 394–401.
(18) Lamprecht, B.; Krenn, J. R.; Schider, G.; Ditlbacher, H.; Salerno, M.; Felidj, N.; Leitner, A.; Aussenegg, F. R.; Weeber, J. C. *Appl. Phys. Lett.* **2001**, *79*, 51–53.
(19) Verhagen, E.; Dionne, J. A.; Kuipers, L.; Atwater, H. A.; Polman, A. *Nano Lett.* **2008**, *8*, 2925–2929.
(20) Ditlbacher, H.; Hohenau, A.; Wagner, D.; Kreibig, U.; Rogers, M.; Hofer, F.; Aussenegg, F. R.; Krenn, J. R. *Phys. Rev. Lett.* **2005**, *95*, 257403.
(21) Sanders, A. W.; Routenberg, D. A.; Wiley, B. J.; Xia, Y. N.; Dufresne, E. R.; Reed, M. A. *Nano Lett.* **2006**, *6*, 1822–1826.
(22) Akimov, A. V.; Mukherjee, A.; Yu, C. L.; Chang, D. E.; Zibrov, A. S.; Hemmer, P. R.; Park, H.; Lukin, M. D. *Nature* **2007**, *450*, 402–406.
(23) Knight, M. W.; Grady, N. K.; Bardhan, R.; Hao, F.; Nordlander, P.; Halas, N. J. *Nano Lett.* **2007**, *7*, 2346–2350.
(24) Manjavacas, A.; García de Abajo, F. J. *Nano Lett.* **2009**, *9*, 1285–1289.
(25) Fang, Y. R.; Wei, H.; Hao, F.; Nordlander, P.; Xu, H. X. *Nano Lett.* **2009**, *9*, 2049–2053.
(26) Li, Z. P.; Hao, F.; Huang, Y. Z.; Fang, Y. R.; Nordlander, P.; Xu, H. X. *Nano Lett.* **2009**, *9*, 4383–4386.
(27) Wei, H.; Ratchford, D.; Li, X. Q.; Xu, H. X.; Shih, C. K. *Nano Lett.* **2009**, *9*, 4168–4171.
(28) Yan, R. X.; Pausauskie, P.; Huang, J. X.; Yang, P. D. *Proc. Natl. Acad. Sci. U.S.A.* **2009**, *106*, 21045–21050.
(29) Shegai, T.; Li, Z. P.; Dadosh, T.; Zhang, Z.; Xu, H. X.; Haran, G. *Proc. Natl. Acad. Sci. U.S.A.* **2008**, *105*, 16448–16453.
(30) Li, Z. P.; Shegai, T.; Haran, G.; Xu, H. X. *ACS Nano* **2009**, *3*, 637–642.
(31) Sun, Y. G.; Mayers, B.; Herricks, T.; Xia, Y. N. *Nano Lett.* **2003**, *3*, 955–960.
(32) Liu, S. D.; Cheng, M. T.; Yang, Z. J.; Wang, Q. Q. *Opt. Lett.* **2008**, *33*, 851–853.
(33) Chang, D. E.; Sorensen, A. S.; Hemmer, P. R.; Lukin, M. D. *Phy. Rev. B* **2007**, *76*, No. 035420.
(34) Gisin, N.; Ribordy, G. G.; Tittel, W.; Zbinden, H. *Rev. Mod. Phys.* **2002**, *74*, 145–195.

DOI: 10.1021/nl100528c | *Nano Lett.* **2010,** *10,* 1831–1835